Available online at www.sciencedirect.com
SCIENCE DIRECT
Polymer 47 (2006) 1732–1740
polymer
www.elsevier.com/locate/polymer

Elastic behavior of compact polymer chain transporting through an infinite adsorption channel

Linxi Zhang [a,*], Jin Chen [b]

[a] Department of Physics, Wenzhou University, Wenzhou 325027, People's Republic of China
[b] Department of Physics, Zhejiang University, Hangzhou 310027, People's Republic of China

Received 12 November 2005; received in revised form 10 January 2006; accepted 11 January 2006

Abstract

The elastic behavior of a single compact chain transporting through an infinite adsorption channel is investigated using the pruned-enriched-Rosenbluth method (PERM). In our model, single compact chain is fixed with one of its first monomer at a position in an infinite adsorption channel, is then pulled slowly along the direction of z-axis. We first calculate the chain size and shape of compact chains transporting through an infinite channel, such as mean-square end-to-end distance per bond $\langle R^2\rangle/N$, mean-square radii of gyration per bond $\langle S^2\rangle/N$, $\langle S^2\rangle_{xy}/N$ and $\langle S^2\rangle_z/N$, and shape factor $\langle\delta\rangle$ for the changes in the size and shape of compact chains during the translocation process. If there are strong adsorption interactions between the monomers and the channel, some special behaviors for the size and shape of compact chains are obtained during the process. On the other hand, some thermodynamics properties are also investigated, such as average energy bond, average Helmholtz free energy per bond, elastic force per bond f and energy contribution to elastic force per bond f_E. During the translocation process, elastic force f is less than zero, and has some plateaus in some special regions for strong adsorption interaction, which may explain how the adsorption interaction drives chains through narrow channels or pores in many biological systems because $f<0$ means that the translocation process need no external force on the chains. These investigations can provide some insights into the mechanics of proteins infiltrating through membrane. In the meantime, by recording and comparing these force-extension curves, we may also investigate the complex interactions between biopolymers (such as protein, RNA, and DNA) and the membranes, and determine indirectly the complicated structure of the channel.

Keywords: Elastic behavior; PERM; Adsorption channel

1. Introduction

The translocation of biopolymers such as RNA, DNA and protein molecules through narrow channels or pores is an important phenomenon in many biological systems and industrial processes. This progress is controlled by membrane proteins, which act as selective channel transporters. Salient examples include the transport of RNA and protein across nuclear pores in order for cell to produce new protein codes [1,2], protein translocation into mitochondria which cannot produce their required proteins and must import them across two protein membranes from cell cytoplasm [3], the injection of phage DNA into bacteria [4,5]. In fact, DNA migration through microfabricated channels and devices [6,7], gene therapy, and drug delivery [8] are widely applied in the biotechnology. Furthermore, this translation phenomenon has been used to distinguish different single homopolymer strands [9], which can offer the tanlatizing prospect of using biological membranes and pores for rapid DNA sequencing or filtering. For this importance and practicability, in recent years there has been much interest in the study of the translocation of biopolymers through different channels. Understanding this process enables us to deepen our comprehension of many fundamental problems in cell biology, and may also contribute to the development of promising biotechnologies.

Using electrophysiology techniques there have been many experimental efforts to directly investigate a single molecule translocation process [10–12]. Especially the experiment scientists have shown that it is possible to drive a single stranded DNA and RNA through a narrow channel (or pores) by applying an electric field [13,14]. As the actual system is more complicated, the translocation mechanisms are not only limited to one certain cause. At the same time, the driving mechanisms for this biopolymer translocation processes have

* Corresponding author. Tel.: +86 571 884 83790; fax: +86 571 879 51328.
E-mail address: lxzhang@hzcnc.com (L. Zhang).

0032-3861/$ - see front matter © 2006 Elsevier Ltd. All rights reserved.
doi:10.1016/j.polymer.2006.01.054

been a subject of intense discussion; such as ratchet mechanisms [15–17], electric fields [18,19] and chemical potential gradients [20–22] and selective adsorption interactions [23,24] were analyzed by experimental and theoretical methods. However, a few studies show that protein translocation across the membrane is significantly affected by the surrounding environments and membrane–protein interactions [25,26].

In this paper, we investigate the elastic process of single compact polymer chains transporting through an infinite adsorption channel and our aim is to know how the attraction interactions influence the translocation process. Our results imply that the translocation of compact polymer chains through a narrow channel is more complicated and this process also includes the stretching of compact polymer chains inside the channel. In the meantime, comparing force-extension curves, which can be obtained directly from atom force microscopy (AFM), we can also investigate the complex interactions between compact polymer chains and the membranes, and the effect of the shape of channel on the translocation of compact polymer chains.

2. Method of calculation

According to the model of a self-avoiding chain of length N on cubic lattice, the total energy of a compact chain with adsorption interactions between the monomers and the channel can be defined as:

$$E = \sum_{i<j} \varepsilon_{ij}\Delta(r_i - r_j) + V \equiv E_C + E_a \tag{1}$$

where ε_{ij} is the contact energy between monomers i and j and r_i represents the three-dimensional coordination (x_i, y_i, z_i) of ith monomer, $\Delta(r_i - r_j) = 1$ if r_i and r_j are adjoining lattice sites with i and j not adjacent along the chain, and $\Delta(r_i - r_j) = 0$ otherwise. Here, we suppose $\varepsilon_{ij} = -1$ (in the unit of k_BT) [27], and therefore the effect of temperature is ignored. The compact polymer chain is important because it is the principal configuration of the native state of globular protein [27]. V in Eq. (1) represents adsorption interactions between compact chains and the channel [28,29], and also in the unit of k_BT. The adsorption interaction of chains is realized by an introduction of attractive potential between the channel inner wall and chain monomers. In Fig. 1, we draw the schematic diagram of compact chains transporting through an infinite adsorption channel along the direction of z-axis. The surface of $z = 0$ divides the infinite adsorption channel into two different parts with the radius of R_1 and R_2 ($R_2 > R_1$), respectively. The channel inner wall and the $z = 0$ surface have adsorption interactions. In our model, one of its first monomer of compact chain is fixed at one position along z-axis and the other monomers are simulated on cubic lattice by the law of self-avoiding chain and not allowed to penetrate through the boundary. Fig. 1(a) and (b) represent two conformations which one of its first monomer is at different positions z_1 and z_2, respectively. When z increases step by step, we can simulate

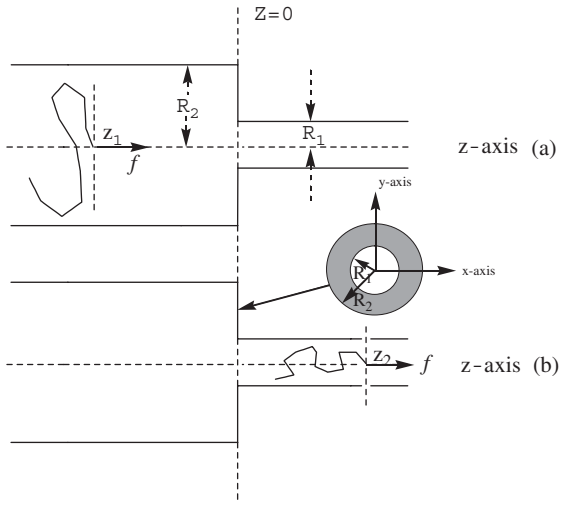

Fig. 1. A model of compact chains transporting through an infinite adsorption channel along the z-axis under the influence of an external force. Here, (a) and (b) represent two conformations of three-dimensional compact chains during the transporting process with one of its first monomer at different positions z_1 and z_2, respectively. R_1 and R_2 represent the radii of the large channel and the small one, respectively.

the translocation process. Of course, if this translocation does not happen spontaneously, we assume that an external force acts on the chain, and pulls the chain along the z-axis direction slowly. Once one monomer is adsorbed on the boundary, there exists a adsorption energy of ε. According to this model, the additional item V in Eq. (1) can be written as:

$$V = \begin{cases} \varepsilon & \text{if} \quad z_i = 0 \quad \text{and} \quad R_1^2 < x_i^2 + y_i^2 < R_2^2 \\ \varepsilon & \text{if} \quad z_i > 0 \quad \text{and} \quad x_i^2 + y_i^2 = R_1^2 \\ \varepsilon & \text{if} \quad z_i < 0 \quad \text{and} \quad x_i^2 + y_i^2 = R_2^2 \\ 0 & \quad\quad\quad\quad \text{elsewise} \end{cases} \tag{2}$$

where (x_i, y_i, z_i) represents the coordination of i-monomer of compact chains ($i = 0,1,2,\ldots,N$), and $\varepsilon < 0$. In the past few years, scientists have shown that for the bacterial α-hemolysin (α-HL), the membrane channel serves as a model system for the translocation process [9–14,30–32]. Thus, this simple model is always adopted for the translocation process of the actual complicated biologic system according to the real shape of membrane. Another reason why we adopt such a model is that the incorporation of membrane proteins into lipid bilayers always occurs spontaneously because there exist different shapes (such as different radii) of channels with varying adsorption energy [30–32]. Our aim here is to investigate how the membrane–protein adsorption interaction drives the compact polymer chain through the channel.

At the same time, the partition function Z is

$$Z = \sum_i \exp(-E_i) \tag{3}$$

where $\sum_i$ is the sum of conformations whose z-axis coordination of one of its first monomer of a chain is z, and E_i is in the unit of k_BT. The partition function is very important, and is widely used to study thermodynamic properties of

polymer chains. As the number of conformations is very large for long compact chains, it is difficult to calculate the partition function by the enumeration calculation method. Here, we use the pruned-enriched-Rosenbluth method (PERM) [33,34] instead. Grassberger used this algorithm for simulating flexible chain polymers and their results illuminate that this method is the most efficient for three-dimensional polymers on the simple-cubic lattice [33]. Therefore, we adopt the PERM to investigate statistical properties of compact chains here.

The Helmholtz free energy of compact chains is derived from the partition function

$$A = -k_B T \ln Z \tag{4}$$

Elastic force f can be obtained from the dependence of A on the elongated distance along the force direction (i.e. z-axis) [35–38]:

$$f = \frac{\partial A}{\partial z} \tag{5}$$

According to Newton's third law, elastic force f is the force which is stored in the compact chains. Energy contribution to the elastic force f_E is also defined as

$$f_E = \frac{\partial < E >}{\partial z} \tag{6}$$

here $\langle E \rangle$ is the average energy of compact chains which is defined in Eq. (1). In fact, elastic behaviors of general polymer chains have been investigated for a long time [37,38]. However, the elastic behavior of polymer chains transporting through an infinite adsorption channel may be different from general polymer chains.

3. Results and discussion

3.1. Chain size and shape

Mean-square end-to-end distance $\langle R^2 \rangle$ is important, and we first plot the characteristic ratio of end-to-end distance $\langle R^2 \rangle / Nb^2$ as a function of z_0 for compact chains transporting through an infinite channel with different radii of the small channel R_1 and different adsorption energy ε in Fig. 2. Here, we employ adsorption interaction energies of $\varepsilon = 0, -1, -3$, and bond length $b = 1$. We define z_0 as

$$z_0 = \frac{z}{N} \tag{7}$$

where z is the z-coordinate of one of its first monomer, and the influence of N may be ignored here if z_0 instead of z. The left-side channel is fixed at the radius of $R_2 = 6$, and the translocation process starts from large channel to small one because the incorporation of membrane proteins into lipid bilayers is always the process of proteins moving from large confinement size to small one. In Fig. 2(a), the curves of $\varepsilon = -3$ are far different from the other cases with $\varepsilon = 0$, and -1. Here, we first discuss the case of $\varepsilon = -3$. At the beginning of elastic process, $\langle R^2 \rangle / N$ changes a little and the value is about 6.33. In fact, when the compact polymer chain is

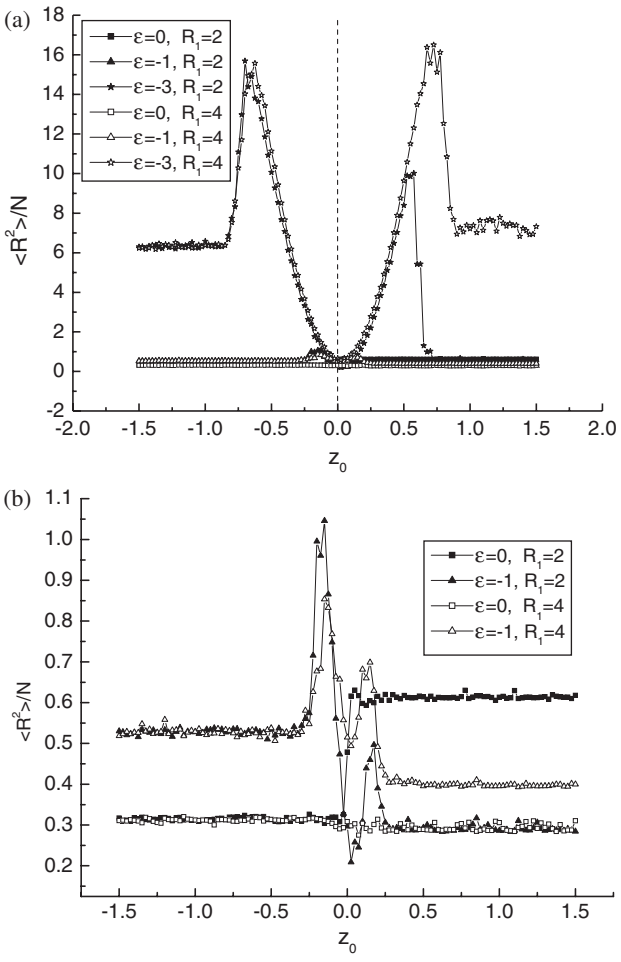

Fig. 2. Characteristic ratio $\langle R^2 \rangle / N$ as a function of z_0 for compact chains with different radii of the small channel R_1 and different adsorption energy ε. Here, $N = 40$ and $R_2 = 6$.

far away from the surface of $z_0 = 0$ (i.e. $z = 0$), it is only attracted by channel inner wall and impossible for any monomers to touch the $z = 0$ surface, therefore the shape and size of polymer chain keeps unchanged. However, there exists an abrupt increase for $\langle R^2 \rangle / N$ from 6.33 to 15.6 in the range of $z_0 = -0.85 \sim -0.65$ for $R_1 = 2$ and 4, respectively. It may be thought that some monomers of compact polymer chains begin to be adsorbed on the $z = 0$ surface when $-0.65 \geq z_0 \geq -0.85$. This $z = 0$ adsorption surface is vertical to the inner wall and the chain can be elongated not only by the channel walls but also the $z = 0$ surface. Therefore, $\langle R^2 \rangle / N$ increases greatly. When we continue to pull the compact chains along the z-axis direction, the characteristic ratio decreases sharply from 15.6 to 0.36 in the range of $z_0 = -0.65$–0.0, and this result is contrary to that in the range of $z_0 = -0.85 \sim -0.65$. This means that when the chain is close to the $z = 0$ surface, the chain is compressed in order to pass through the narrow channel. Furthermore, when $z_0 < 0$, the curves with solid and hollow star symbols are almost identical. After compact polymer chains are pulled through the $z = 0$ surface, $\langle R^2 \rangle / N$ increases to another maximum again. Because of the effect of small radius R_1, the characteristic ratio reaches a maximum of 10.0 at $z_0 = 0.575$ for

$R_1=2$ while the value climbs to another maximum of 16.5 at $z_0=0.725$ for $R_1=4$. Here, we select the case of $R_1=2$ because it is representative. For small radius of $R_1=2$, the compact chain is easy to be adsorbed on the inner wall. Therefore, $\langle R^2\rangle/N$ decreases to the value of 0.47 when $z_0=0.575$. Although one of its first monomer has passed through the $z=0$ surface, the other monomers are still adsorbed on the $z=0$ surface. Only after passing through $z_0=0.575$, is the compact chain free from the restriction of the $z_0=0$ surface and it reaches the stable value of 0.47 even if z_0 increases again. If $R_1=4$, the position of maximum value of $\langle R^2\rangle/N$ is $z_0=0.725$ and the stable value of$\langle R^2\rangle/N$ becomes 7.32. Comparing with these three stable values for $R_1=2$, 4 and $R_2=6$, we can find the results do not change monotonously with the increasing of channel radius. On the other hand, in order to show the results of $\varepsilon=0$, and -1 in more detail, we plot them in Fig. 2(b). When $\varepsilon=0$, two curves with square symbols are all about 0.31 when $z_0<0$, and they become 0.61 and 0.29 for $R_1=2$ and 4, respectively when $z_0>0$. It is obvious that under this condition the shape of chain is only related to the channel radii of R_1 and R_2. $\langle R^2\rangle/N$ changes a little except for the range of $z_0=-0.85\sim0.575$. Otherwise, the compact chain keeps a constant value of $\langle R^2\rangle/N$. The change of the chain size reflects the change of the shape of channel. Therefore, we can predict the shape of protein membrane from $\langle R^2\rangle/N$ as a function of z_0 during this process.

We also calculate the perpendicular ($\langle S^2\rangle_{xy}$) and parallel ($\langle S^2\rangle_z$) mean square radii of gyration of compact chains, which are defined as:

$$\langle S^2\rangle_{xy}=\left\langle\frac{1}{N+1}\sum_{i=0}^{N}\left[(x_i-c_{\rm cm})^2+(y_i-y_{\rm cm})^2\right]\right\rangle \tag{8}$$

$$\langle S^2\rangle_z=\left\langle\frac{1}{N+1}\sum_{i=0}^{N}(z_i-z_{\rm cm})^2\right\rangle \tag{9}$$

$$\langle S^2\rangle=\langle S^2\rangle_{xy}+\langle S^2\rangle_z, \tag{10}$$

where $(x_{\rm cm}, y_{\rm cm}, z_{\rm cm})$ is the position of the center of a compact chain, and the angular brackets $\langle\,\rangle$ denote thermodynamic average. $\langle S^2\rangle/N$, $\langle S^2\rangle_{xy}/N$ and $\langle S^2\rangle_z/N$ as a function of z_0 for compact chains transporting through an infinite channel with different channel radii R_1 and different adsorption energy ε are shown in Fig. 3. $\langle S^2\rangle/N$ is shown in Fig. 3(a), and the curves with strong adsorption interaction are completely different from the others. We first discuss the case of $\varepsilon=-3$. When $z_0<-0.85$, the ratio of $\langle S^2\rangle/N$ keeps a stable of 0.87. This range is consistent with the results in Fig. 2. With the increasing of z_0, the curves do not change monotonously, so the ratio first increases to 2.0 at $z_0=-0.65$ and then decreases to the minimum at $z_0=0$. When z_0 is close to 0, $\langle S^2\rangle/N$ becomes 0.11 and 0.18 for $R_1=2$ and 4, respectively. If compact chains are pulled through the surface of $z_0=0$ and into the small channel (i.e. $z_0>0$), $\langle S^2\rangle/N$ first keeps unchanged in small range, then increases abruptly and decreases again, until it keeps a stable value. When $\varepsilon=0$, $\langle S^2\rangle/N$ changes from 0.093 ($z_0<0$) to 0.11 ($z_0>0$) for $R_1=2$. The result of $\varepsilon=-1$ is quite similar to

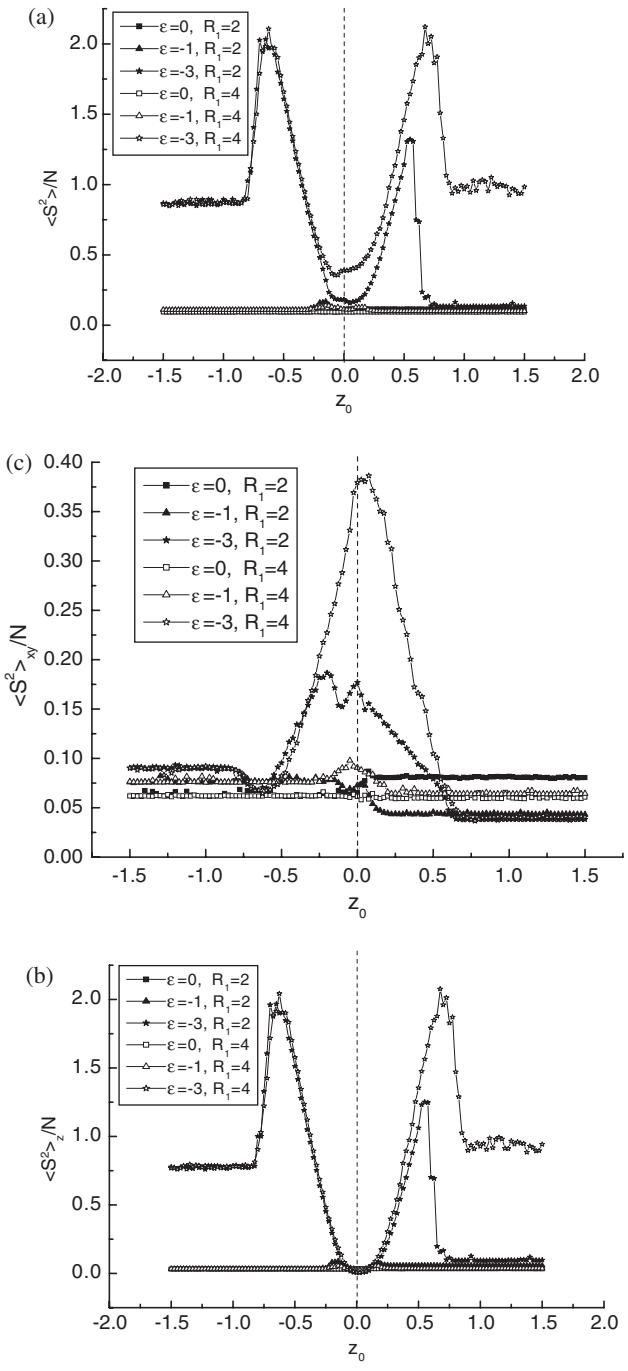

Fig. 3. Mean-square radii of gyration per bond $\langle S^2\rangle/N$ (a), $\langle S^2\rangle_{xy}/N$ (b), and $\langle S^2\rangle_z/N$ (c) as a function of z_0 for compact chains with different radii of the small channel R_1 and different adsorption energy ε. Here, $N=40$ and $R_2=6$.

$\varepsilon=-3$, and it changes less than that of $\varepsilon=-3$. In our model, the direction of force acting on the chain is along the z-axis, so the change of shape is different in three directions, i.e. x, y, and z-axis. In order to analyze this elastic process completely, we also calculated $\langle S^2\rangle_{xy}/N$ and $\langle S^2\rangle_z/N$, and the results are shown in Fig. 3(b) and (c). The result of $\langle S^2\rangle_z/N$ is similar to $\langle S^2\rangle/N$, however, $\langle S^2\rangle_{xy}/N$ is different from $\langle S^2\rangle/N$.

In order to investigate the shape of compact chains in more detail, we here consider the radius of gyration tensor S, which is defined as:

$$S = \frac{1}{N+1}\sum_{i=0}^{N} S_i S_i^T = \begin{pmatrix} S_{xx} & S_{xy} & S_{xz} \\ S_{yx} & S_{yy} & S_{yz} \\ S_{zx} & S_{zy} & S_{zz} \end{pmatrix}. \quad (11)$$

Here, $S_i = \mathrm{col}(x_i, y_i, z_i)$ is the position of monomer i in a frame of reference with its origin at the center of a chain. The tensor S can be diagonalized to form a diagonal matrix with three eigenvalues L_1^2, L_2^2 and L_3^2 $(L_1^2 \le L_2^2 \le L_3^2)$. Solc and Stockmayer first used these parameters $\langle L_1^2\rangle : \langle L_2^2\rangle : \langle L_3^2\rangle$ to measure the shape of flexible polymer chains [39,40], and they estimated the ratio to be 1:2:7:11.7 based on a random walk of 100 bonds on a simple cubic lattice using Monte Carlo (MC) technique. According to three eigenvalues from Eq. (11), another parameter [41,42] of the shape of chain can be obtained by combining the reduced components to a single quantity that varies between 0 (sphere) and 1 (rod):

$$\langle\delta\rangle = 1 - 3\left\langle \frac{L_1^2L_2^2 + L_2^2L_3^2 + L_1^2L_3^2}{(L_1^2 + L_2^2 + L_3^2)^2} \right\rangle \quad (12)$$

$\langle\delta\rangle$ as a function of z_0 for compact chains with different channel radii R_1 and different adsorption energy ε are shown in Fig. 4. The value of $\langle\delta\rangle$ for general compact polymer chain without confinement should be zero, and it is a sphere. When $\varepsilon = 0$, our result is 0.15 for $R_1 = 4$, while the value is 0.15 with $z_0 < 0$ and 0.22 with $z_0 > 0$ for $R_1 = 2$. Those values are all greater than zero. The reason may be that in our model the compact chain has been compressed a little by the confinement condition. If the channel radius is large enough, the compact chains can come back to the globule shape. If there exist strong adsorption interaction, the results are more complex. For $\varepsilon = -3$, $\langle\delta\rangle$ is equal to 0.71 when $z_0 < -0.85$, and the shape is close to a rod. The reason may be that most of monomers are attracted by the channel adsorption inner wall, so the shape looks like a rod parallel to the z-axis. When we pull the compact chains slowly towards the surface of $z_0 = 0$, for example, from $z_0 = -0.85$ to -0.65, $\langle\delta\rangle$ increase from 0.71 to 0.90. At this point, some monomers begin to be attracted by the surface of $z_0 = 0$, so the shape changes abruptly and the chains are compressed in the xy-plane. If we continue to pull compact chains along the z-axis, $\langle\delta\rangle$ decreases abruptly from 0.91 to 0.12. When the compact chain is close to the surface of $z_0 = 0$, the shape of compact chains is almost the globule. In order to show the change of the shape in more detail, we add five sketch maps in five different regions in Fig. 4. If the adsorption interaction is $\varepsilon = -1$, different results are obtained in Fig. 4.

Here, we analyze the change of the chain shape and size in order to discuss the effects of different adsorption interaction during the elongation process for compact chains transporting through infinite channel. We can get two conclusions: (1) The behavior of compact chains without adsorption interaction is far different from that with adsorption interaction during this process. (2) The adsorption interaction affects the shape and size deeply, especially for strong adsorption interaction.

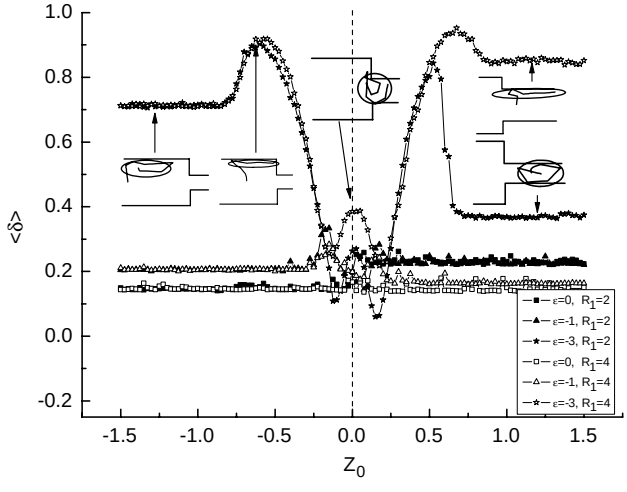

Fig. 4. $\langle\delta\rangle$ as a function of z_0 for compact chains with different radii of the small channel R_1 and different adsorption energy ε. Here, $N = 40$ and $R_2 = 6$.

3.2. Thermodynamics properties

We first investigate average Helmholtz free energy per bond of compact chains during the elongation process. In Fig. 5, we plot average Helmholtz free energy per bond $\langle A\rangle$ as a function of z_0 for compact chains with different channel radii R_1 and different adsorption energy ε. Here, $\langle A\rangle = A/N$ When $\varepsilon = 0$, average Helmholtz free energy per bond is -1.97 $(z_0 < 0)$ and -1.87 $(z_0 > 0)$ for $R_1 = 2$, while it keeps unchanged during the whole process for $R_1 = 4$. These results explain that if the channel has no interaction with compact chains, it is more difficult for compact chains to move spontaneously from large confinement size to small one. When there is the weak attraction of $\varepsilon = -1$, for small radius of $R_1 = 2$, $\langle A\rangle$ remains -1.97 for $z_0 < -0.25$, and then decreases from -1.97 to -2.46 with z_0 increasing, until it increases to -2.34. However, for large radius of $R_1 = 4$, the change of $\langle A\rangle$ during this process is smaller than that for small radius or $R_1 = 2$. Our results can explain how proteins transport through the channel in the membrane by the adsorption interaction for the real

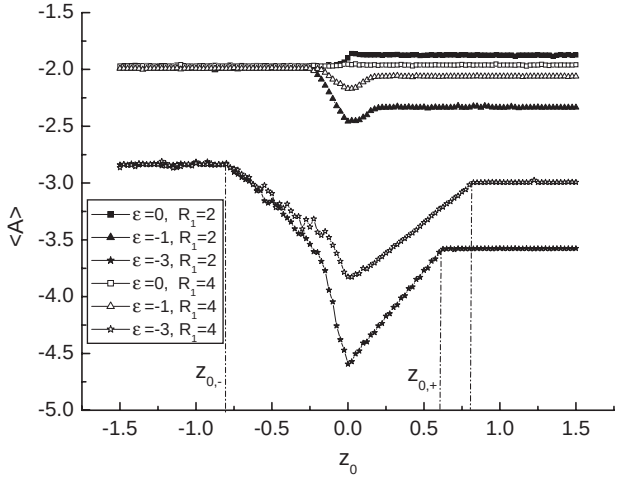

Fig. 5. Average helmholtz free energy per bond $\langle A\rangle$ as a function of z_0 for compact chains with different radii of the small channel R_1 and different adsorption energy ε. Here, $N = 40$, and $R_2 = 6$. $z_{0,-}$ and $z_{0,+}$ represent two turning points for $z_0 < 0$ and $z_0 > 0$, respectively.

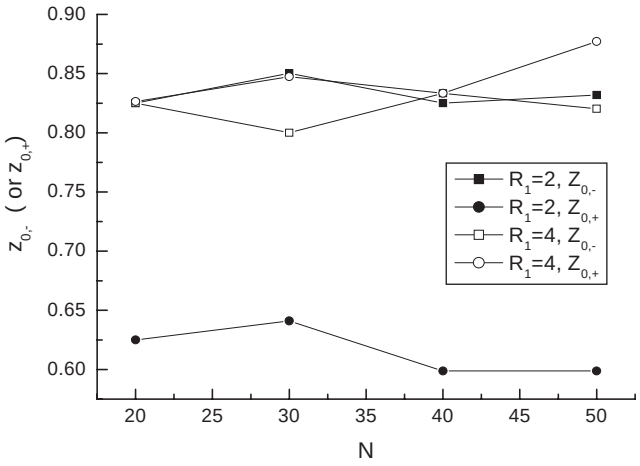

Fig. 6. Turning position $z_{0,-}$ (or $z_{0,+}$) as a function of chain length N for compact chains with different radii of the small channel R_1 and different adsorption energy ε. Here, $R_2=6$.

biologic system. If one of its first monomer passes through the surface of $z_0=0$, there would be a reverse process in which it needs an external force to pull the chain sequentially until the whole compact polymer chain enters the small channel completely. This tendency is more obvious when $\varepsilon=-3$. Here, we define two turning points $z_{0,-}$ and $z_{0,+}$ from which $\langle A\rangle$ begins to change ($z_{0,-}$) and $\langle A\rangle$ begins to keep unchanged ($z_{0,+}$) (see Fig. 5). In Fig. 6, we show the results of turning position $z_{0,-}$ ($z_{0,+}$) as a function of chain length N with different channel radii of R_1. Here, the chain length is from 20 to 50, $\varepsilon=-3$, and we find that both $z_{0,-}$ and $z_{0,+}$ are independent of chain length N.

Average total energy per bond $\langle E\rangle$, average attractive energy $\langle E_a\rangle$, and average contact energy $\langle E_C\rangle$ as a function of z_0 for compact chains with different channel radii of R_1 and different adsorption energy ε are shown in Fig. 7. In Fig. 7(a), the curves of total energy per bond $\langle E\rangle$ for compact chains without adsorption interaction energy are parallel to the x-axis except for the region of $z_0=0$, and $\langle E\rangle$ for $R_1=2$ is slightly greater than that for $R_1=4$. When it is the weak adsorption interaction, (i.e. $\varepsilon=$-1), $\langle E\rangle$ keeps unchanged for $z_0<-0.22$, and decreases as z_0 increases in the range of -0.22–0. It reaches the minimum at $z_0=0$, then increases with z_0 in the range of $0.0<z_0<0.22$, until it keeps unchanged again when $z_0>0.22$. When adsorption interaction energy becomes -3, the total energy per bond $\langle E\rangle$ is stronger than in the other cases, and the curves with star symbols are ladder-shaped. In fact, the total energy includes adsorption interaction energy and contact interaction energy (see Eq. (1)), so we also plot average attractive energy per bond $\langle E_a\rangle$ and average contact energy per bond $\langle E_C\rangle$ in Fig. 7(b) and (c), respectively. In Fig. 7(b), the curve of $\langle E_a\rangle$ is similar to $\langle E\rangle$, especially for strong adsorption energy of $\varepsilon=-3$, and the ladder shape is more obvious. However, in Fig. 7(c), the curves of $\langle E_C\rangle$ are different from $\langle E\rangle$ or $\langle E_a\rangle$, especially when $\varepsilon=-3$. In the range of $-0.85\sim-0.65$, contact energy per bond $\langle E_C\rangle$ for $\varepsilon=-3$ increases slightly. From the above discussion about the shape and size, we know that the monomers in the chain may be attracted by the inner wall

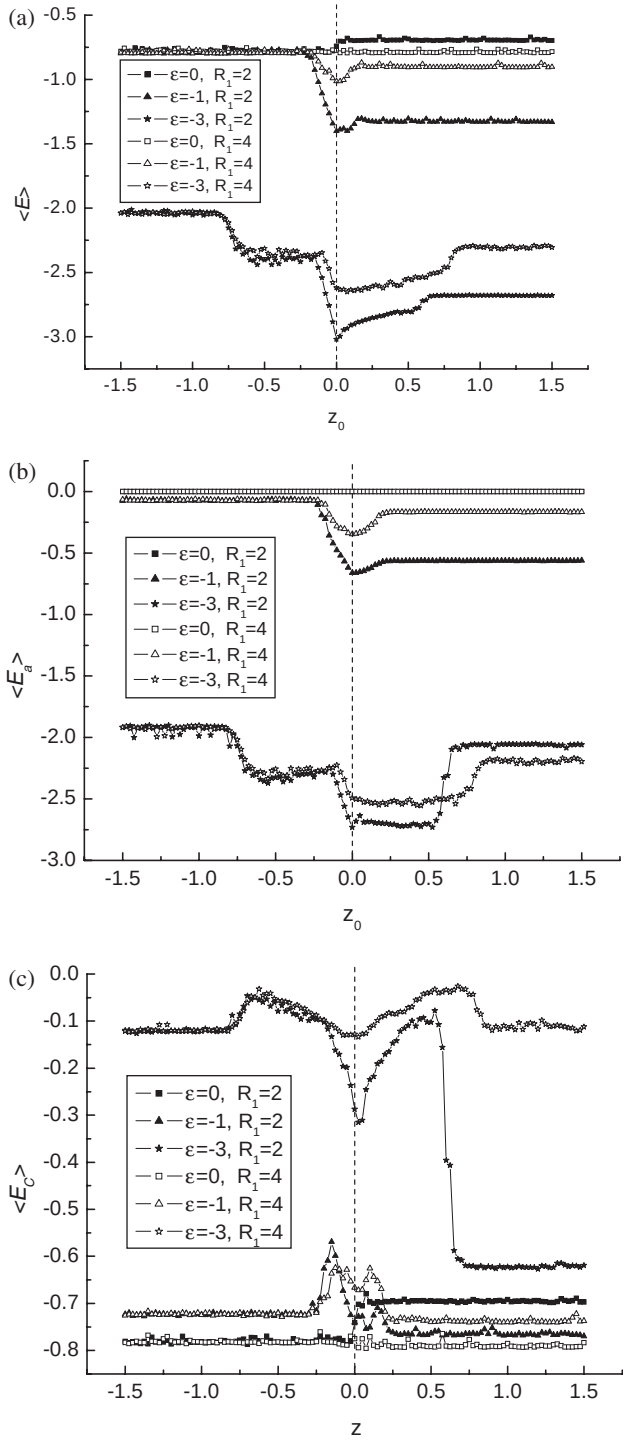

Fig. 7. Average energy per bond as a function of z_0 for compact chains with different radii of the small channel R_1 and different adsorption energy ε. Here, $N=40$ and $R_2=6$. (a) total energy per bond $\langle E\rangle$; (b) adsorption energy per bond $\langle E_a\rangle$; and (c) contact energy per bond $\langle E_C\rangle$.

and the $z=0$ surface. If the chain is elongated, the distance between monomers may increase, and the number of contacts decreases. However, when the compact chain is close to the surface of $z_0=0$, the shape is compressed so that the number of contacts may increase accordingly.

In order to discuss the adsorption-driving, we calculate elastic force f and energy contribution to elastic force f_E according to

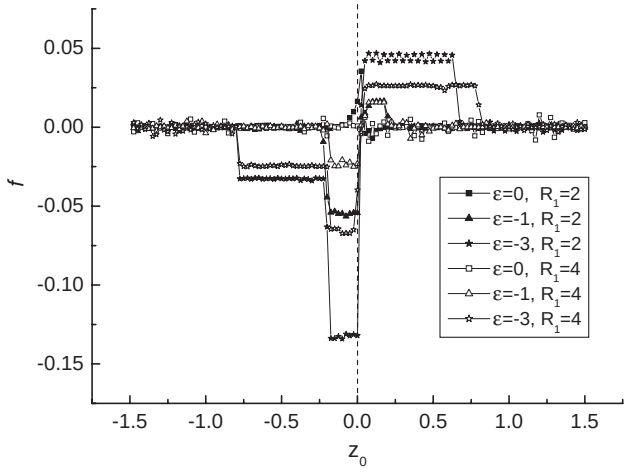

Fig. 8. Elastic force per bond stored in the compact chains (f) as a function of z_0 for compact chains transporting through an infinite channel with different radii of the small channel R_1 and different adsorption energy ε. Here, $N=40$, and $R_2=6$. For example, $f=1$ means $f=42$ pN here if bond length $b=0.1$ nm and temperature $T=300$ K.

Eqs. (5) and (6). In Fig. 8, we plot elastic force f as a function of z_0 for compact chains with different channel radii R_1 and different adsorption energy ε. From Fig. 8, we can find that elastic force is close to zero when $\varepsilon=0$, and this means under this condition no force is needed. When $\varepsilon=-1$, f has two short plateaus with the values of -0.055 and 0.016 in the range of $z_0=-0.22\sim0.0$ and $z_0=0.0\sim0.22$ for $R_1=2$, respectively, and for $R_1=4$, these plateaus become blurry. We all know that if $f<0$, this means that the chains can move spontaneous along the z-axis, and $f>0$ otherwise. When $\varepsilon=-3$, f has six plateaus with the values of -0.033, -0.13 and 0.044 in the ranges of $z_0=-0.78\sim-0.22$, $-0.22\sim0.0$, and $0.0\sim0.63$ for $R_1=2$, respectively, and the values of -0.024, -0.064 and 0.026 in the ranges of $z_0=-0.78\sim-0.22$, $-0.22\sim0.0$, and $0.0\sim0.77$ for $R_1=4$, respectively. From many negative plateaus in Fig. 8, we can get the conclusion that the adsorption interaction is one of the driving mechanisms. Strong adsorption interaction and obvious difference of radii between two side channels can make the chain to move more spontaneously. However, they need strong elastic force to pull the chain continuously after transporting through the surface of $z_0=0$. Single-molecule force spectroscopy (SMFS), based on atomic force microscopy AFM [43], has become a versatile platform in studying intermolecular and intra–molecular interactions with its extremely high force sensitivity [44]. Using SMFS, a number of interacting topics such as protein unfolding, force-induced conformational transitions, host–guest interactions, single-polymer chain elasticity, and single-chain desorption from a substrate have been investigated. In fact, it is very important to investigate the interactions between biopolymers and the translocation channel because it is of fundamental importance both in basic science and in biotechnology. Technological applications of biopolymer-channel interactions include gel permeation chromatography [45] and the use of protein pores as components of biosensors [46,47]. In the meantime, comparing with the experimental results of force-extension curves based on SMFS and our theoretical results, we can also determine the interactions between compact polymer chains and the membrane channels. For example, the interactions between them in fact are more complicated, and the additional item V in Eq. (1) should be expressed in the more general form of

$$V=\begin{cases}\varepsilon_1(z_i) & \text{if } z_i=0 \text{ and } & R_1^2<x_i^2+y_i^2<R_2^2\\ \varepsilon_2(z_i) & \text{if } z_i>0 \text{ and } & x_i^2+y_i^2=R_1^2\\ \varepsilon_3(z_i) & \text{if } z_i<0 \text{ and } & x_i^2+y_i^2=R_2^2\\ 0 & & \text{elsewise}\end{cases} \tag{13}$$

Different expression of V can produce different force-extension curves, and there exists a single corresponding relationship between adsorption energy and force-extension curve. By comparing this relationship, we can determine indirectly the interactions between compact polymer chains and the inner wall. On the other hand, statistical properties of compact chains also depend on the shape of channels. Therefore, we can also determine indirectly the shape of channels by considering these force-extension curves. In Fig. 9, we give an explanation

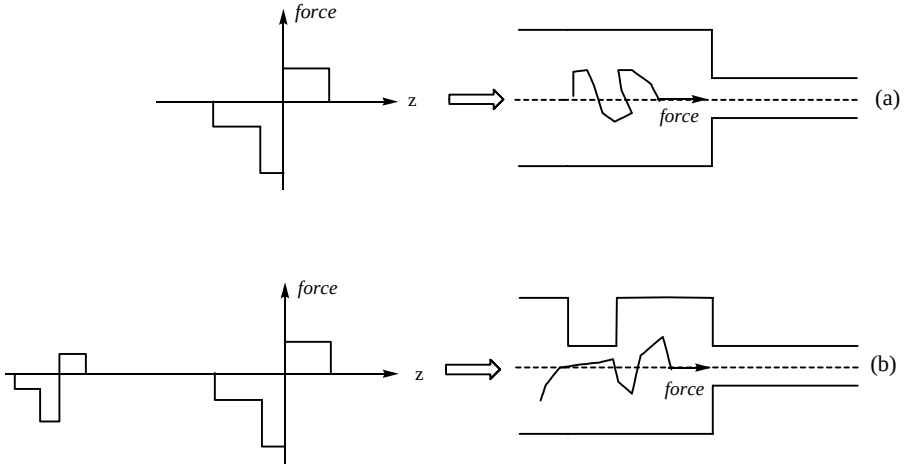

Fig. 9. Prediction of the shape of the channel from the force-extension curve, i.e. force (f)$\sim z$. Here, (a) and (b) represent two cases of different channel shape. Comparing with these force-extension curves, we can determine the shape of channel.

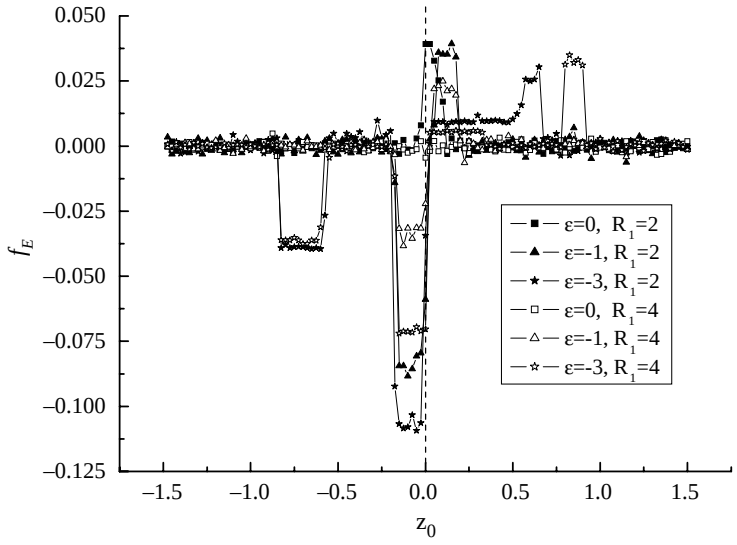

Fig. 10. Energy contribution to elastic force per bond f_E as a function of z_0 for compact chains transporting through an infinite channel with different radii of the small channel R_1 and different adsorption energy ε. Here, $N=40$, and $R_2=6$.

how to determine the shape of channels. In the left of Fig. 9(a), it is a force-extension curve, and in the right of Fig. 9(a), it is the shape of the channel and there exists a corresponding relationship between them. If we can determine the force-extension curve such as the left of Fig. 9(b) using experimental method, we can decide the shapes as similar to that in the right of Fig. 9(b). In the meantime, we can also discuss the driving force in biopolymers moving through protein membranes or holes such as molecular motor [48]. Of course, there are also many intangible questions for us in this field now. In Fig. 10, it is f_E as a function of z_0 for compact chains with different channel radii R_1 and different adsorption energy ε. Similar curves to Fig. 8 can be seen in this figure. There are also several plateaus during the transporting process and these plateaus also fluctuate with different adsorption energy and different channel radii. Through our calculation, we find that the compact polymer chain can voluntarily move with the adsorption interactions, which prove that the adsorption interaction is one of the driving forces in the translation of proteins. This investigation can provide some insights into the elastic behavior of proteins through narrow channels or pores.

Acknowledgements

This research was financially supported by National Natural Science Foundation of China (Nos. 20274040, 20574052), Program for New Century Excellent Talents in University, and Natural Science Foundation of Zhejiang Province (Nos. R404047, Y405011, Y405553). We thank the referees for their critical reading of the manuscript and their good ideas.

References

[1] Alberts B, Bray D, Lewis J, Raff M, Roberts K, Watson JD. Molecular biology of the cell. New York: Garland; 1994.
[2] Bustamante JO, Hanover JA, Liepins A. J Membr Biol 1995;146:239–51.
[3] Simon SM, Blobel G. Cell 1991;65:371–80.
[4] Chacinska A, Pfanner N, Meisinger C. Trends Cell Biol 2002;12: 299–303.
[5] Drieselkelmann B. Microbiol Rev 1994;58:293–316.
[6] Han J, Turner SW, Craighead HG. Phys Rev Lett 1999;83:1688–91.
[7] Turner SWP, Calodi M, Craighead HG. Phys Rev Lett 2002;88:128103.
[8] Chang DC. Guide to electroporation and electrofusion. New York: Academic; 1992.
[9] Meller A, Nivon L, Brandin E, Golovchenko J, Branton D. Proc Natl Acad Sci USA 2000;97:1079–84.
[10] Henrickson SE, Misakian M, Robertson B, Kasianowicz JJ. Phys Rev Lett 2000;85:3057–60.
[11] Howorka S, Movileanu L, Lu X, Magnon M, Cheley S, Braha O, et al. J Am Chem Soc 2000;122:2411–6.
[12] Kasianowicz JJ, Henrickson SE, Weetall HH, Robertson B. Anal Chem 2001;73:2268–72.
[13] Kasianowicz JJ, Brandin E, Branton D, Deamer DW. Proc Natl Acad Sci USA 1996;93:13770–3.
[14] Meller A, Nivon L, Branton D. Phys Rev Lett 2001;86:3435–8.
[15] Schalz G, Dobberstein B. Science 1996;271:1519–20.
[16] Simon SM, Peskin CS, Oster GF. Proc Natl Acad Sci USA 1992;89: 3770–4.
[17] Slater GW, Guo HL, Nixon GI. Phys Rev Lett 1997;78:1170–3.
[18] Lubensky DK, Nelson DR. Biophys J 1999;77:1824–38.
[19] Slonkina E, Kolomeisky AB. J Chem Phys 2003;118:7112–8.
[20] diMarzio EA, Mandell AL. J Chem Phys 1997;107:5510–4.
[21] Muthukumar M. J Chem Phys 1999;111:10371–4.
[22] Tian P, Smith GD. J Chem Phys 2003;119:11475–83.
[23] Park PJ, Sung W. J Chem Phys 1998;108:3013–8.
[24] Milchev A, Binder K, Bhattacharya A. J Chem Phys 2004;121:6042–51.
[25] Sung W, Park PJ. Phys Rev Lett 1996;77:783–6.
[26] Baumgartner A, Skolnick J. Phys Rev Lett 1995;74:2142–5.
[27] Chan HS, Dill KA. Macromolecules 1989;22:4559–73.
[28] Zhang LX, Chen J. Polymer 2005;46:6208–15.
[29] Chen J, Zhang LX. Colloids Surf, A Physicochem Eng Aspects 2005;260: 137–44.
[30] Akeson M, Brantion D, Kasianowicz J, Brandin E, Deamer D. Biophys J 1999;77:3227–33.
[31] Howorka S, Movileanu L, Braha O, Bayley H. Proc Natl Acad Sci USA 2001;98:12996–3001.

[32] Mathe J, Aksimentiev A, Nelson DR, Schulten K, Meller A. Proc Natl Acad Sci USA 2005;102:12377–82.
[33] Grassberger P. Phys Rev E 1997;56:3682–93.
[34] Combe N, Vlugt TJH, Wolde PRT, Frenkel D. Molecular Phys 2003;101: 1675–82.
[35] Sun TT, Zhang LX, Chen J, Shen Y. J Chem Phys 2004;120:5469–76.
[36] Zhang LX, Jiang ZT, Zhao DL. J Polym Sci, Part B: Polym Phys 2002;40: 105–12.
[37] Curro JG, Mark JE. J Chem Phys 1984;80:4521–5.
[38] Mark JE. J Phys Chem B 2003;107:903–13.
[39] Solc K, Stockmayer WH. J Chem Phys 1971;54:2756–7.
[40] Solc K. J Chem Phys 1971;55:335–44.
[41] Zifferer G, Preusser W. Macromol Theory Simul 2001;10:397–407.
[42] Jagodzinski O, Eisenriegler E, Kremer K. J Phys I 1992;2:2243–79.
[43] Hansma HG, Hoh JH. Annu Rev Biophys Biomol Struct 1994;23: 115–40.
[44] Hugel T, Seitz M. Macromol Rapid Commun 2001;22:989–1016.
[45] Liu L, Li P, Asher SA. Nature 1999;397:141–4.
[46] Bayley H, Cremer PS. Nature 2001;413:226–30.
[47] Bayley H, Braha O, Gu LQ. Adv Matter 2000;12:139–42.
[48] Chacinska A, Pfanner N, Meisinger C. Trends Cell Biol 2002;12: 299–303.